Computational Modeling of Electromagnetically Induced Heating of Magnetic Nanoparticle Materials for Hyperthermic Cancer Treatment

L. Rast* and J.G. Harrison**

* University of Alabama at Birmingham, Birmingham, AL, USA, laurenr@uab.edu
** University of Alabama at Birmingham, Birmingham, AL, USA, jgharrison@uab.edu

ABSTRACT

We present results on the computational modeling of electromagnetically induced heating for the purpose of hyperthermic cancer treatment with magnetic nanoparticle fluids. Magnetic nanoparticle hyperthermia can be used for direct targeting and destruction of tumors through heat treatment or as a complement to chemotherapy. The use of ferrofluids for cancer treatment requires that appreciable volumetric heating power be generated, while maintaining safe values of frequency and magnetic field strength and reducing the risk of spot heating healthy tissue. It is necessary to determine an ideal range of input parameters for the complex magnetic susceptibility of the ferrofluid and the magnitude of the driving magnetic field. We do this by the coupling of the solution of Maxwell's equations in a model of the tumor and surrounding tissue as input to the Pennes Bioheat Equation (PBE). Both sets of equations are solved via the Finite Difference Time Domain (FDTD) Method.

Keywords: hyperthermia, cancer treatment, nanotechnology, computational modeling, ferrofluid

1 INTRODUCTION

Hyperthermia therapy for cancer is a medical treatment in which tissue temperatures are elevated, usually to a value of at least 41^0C, for the purpose of damaging or destroying cancer cells. Hyperthermic cancer treatment is advantageous due to fewer side effects than traditional chemotherapy or radiotherapy. Magnetic materials under the influence of an AC magnetic field are particularly convenient for hyperthermic applications. Magnetic nanoparticle systems can be utilized both as drug delivery agents for chemotherapy and for direct targeting and destruction of tumors through heat treatment. Additionally, since these are nanoscale materials, the energy deposition in the cancer cells would be extremely localized. Surrounding tissue would therefore incur minimal damage, making these systems superior to traditional hyperthermic treatment. Since investigation of the applications of magnetic materials for hyperthermia began in 1957, a wide variety of magnetic materials, field strengths, and frequencies have been used in these experiments [1]. Human clinical trials have recently begun as a result of the increased safety and efficacy of magnetic nanomaterials for hyperthermia [2]. The subject of this research is the computational modeling of electromagnetic and thermal effects during the hyperthermic treatment of cancer using magnetic nanoparticles systems, particularly ferrofluids. The goal of these calculations is to determine an ideal range of magnetic field strengths and frequencies, and magnetic susceptibilities for the ferrofluid.

A sustained temperature above 41^0C can cause irreversible damage to cell function leading to apoptosis as well as heat-induced sensitization of cells to radiation and some cytotoxic drugs. A sustained temperature above 45^0C causes other forms of cell death, commonly referred to as necrosis [3][4][5]. Apoptotic cell death occurs in a controlled manner and therefore, in contrast to other forms of cell death, does not lead to inflammitory responses and lysis of cells, which damage the overall health of the organism [5][6]. Localized hyperthermia should therefore ideally heat cancerous tissue to temperatures between 41^0C and 45^0C while maintaining temperatures below 41^0C within the healthy tissue.

The safe and useful range of magnetic field strengths and frequencies for these applications are considered to be $0 < H < 15$ kA/m and $0.05 < f < 1.2$ MHz. Higher field strengths can lead to problems including aggregation of magnetic materials, leading to embolisms. Lower frequencies can cause stimulation of the skeletal or peripheral muscles, or even stimulation of the cardiac muscles and arrhythmias. It has also been established that exposure to fields where the product $H_0 \cdot f$ is less than $4.85 \cdot 10^8$ $Am^{-1}s^{-1}$ (where H_0 is the magnitude of the applied magnetic field) is safe for use in humans [7]. This restriction limits tissue heating power and may be relaxed depending on the diameter of the region being treated and the severity of the illness. We assume a weaker criterion $H_0 \cdot f < 5 \cdot 10^9$ $Am^{-1}s^{-1}$ in our calculations [7][8].

In addition to the restrictions on these input parameters mentioned in previous sections, one must also consider the delivery of the magnetic nanoparticles to the tumor region. This is of particular concern for the treatment of deep-seated brain tumors, where direct injection of the magnetic material to the tumor site is impractical. In order to cross the blood-brain barrier or blood-

brain-tumor barrier, particles must be quite small (12 nm magnetic core size to cross the blood-brain-tumor barrier) [9].

In order to determine a safe range of parameters where the risk of spot heating of the healthy tissue is minimized, yet appreciable volumetric heating power is generated, it is necessary to determine a set of ideal input parameters, including H_0, f, and material properties of the ferrofluid.

2 THEORY

2.1 Power Loss Due to Inductive Heating

An electrically conductive body subject to an AC magnetic field will have induced electrical currents that give rise to heating due to the resistance of the material. Smythe found an analytical expression for the time averaged power dissipation of an inductively heated sphere [10]. If it is assumed that the particles are smaller than the domain size, and $\mu = \mu_0$ (we use SI units throughout), the Smythe formula simplifies. The subsequent series expansion (after multiplication by the number of spheres in a sample, $n = 3\pi/4\phi R^3$, where ϕ is the volume fraction of nanoparticles in the fluid) then yields the time-averaged power dissipation per unit volume:

$$P = \frac{\phi\sigma(\pi RBf)^2}{5} \tag{1}$$

(1) applies to small particles and is valid for frequencies much less than the critical frequency, f_c (at f= f_c the radius of the sphere is equal to the skin depth), where

$$f_c = \frac{1}{\pi R^2 \mu_0 \sigma} \tag{2}$$

$\sigma \equiv$ electrical conductivity = 200 $\Omega^{-1}\text{cm}^{-1}$ for magnetite, so $f_c = 5 \cdot 10^{17}$ Hz for R = 5 nm, then if B = 0.06 T and $\phi = 0.071$ (typical values for clinical hyperthermia with a ferrofluid), $P = 2.5 \cdot 10^{-10}\text{Wcm}^{-3}$. If instead, $\sigma = 9.3 \cdot 10^4 \Omega^{-1}\text{cm}^{-1}$ (for iron), $P = 1.2 \cdot 10^{-7}\text{Wcm}^{-3}$. Since appreciable heating occurs due to magnetic nanoparticle fluid hyperthermia, there must be some heating mechanism other than induction for these materials [11].

2.2 Power Loss Due to Brownian and Néel Relaxation

The heating processes for magnetic nanoparticle fluids were first detailed by Rosensweig based on the Debye model for dielectric dispersion in polar fluids [12]. When an alternating magnetic field is applied to a ferrofluid, the magnetic moments of the magnetic nanoparticles rotate to align with the changing applied field. As the magnetic field decreases, the magnetic moments rotate back to their equilibrium positions. Rotation of the particles in the viscous medium (Brownian relaxation) and rotation of the magnetic moments within the crystal (Néel relaxation) both result in power dissipation due to friction. A phase lagging between the applied magnetic field and rotation of the magnetic moments results in frictional heating. High heating rates are achieved in the regime of particle size where the Néel mechanism does not dominate the relaxation processes.

The volumetric heating power (P) of a ferrofluid due the phase lag between the applied field and the magnetization (and therefore a nonzero value for χ'') is given by [12]:

$$P = \mu_0 \pi \chi'' f H_0^2 \tag{3}$$

Where $\chi \equiv$ complex magnetic susceptibility of the ferrofluid = $\chi' + i\chi''$. χ'' depends upon many material properties of the ferrofluid, including the the nanoparticle size and size distribution, the volume fraction of nanoparticles in the fluid, the domain magnetization of the suspended particles, the saturation magnetization of the ferrofluid, the viscosity of the fluid, and the frequency of the applied magnetic field [12].

Measurements of the heat generation from magnetic particles are most often quoted in terms of the specific absorption rate (SAR), which has units of W/g. Since equation (3) gives the volumetric heating power of a ferrofluid, the specific absorption rate (SAR) is given by:

$$P = SAR \times \rho_m \tag{4}$$

where ρ_m is the density of the ferrofluid. Ferromagnetic materials require extremely high field strengths ($\approx 100\text{kAm}^{-1}$) before they approach a fully saturated hysteresis loop. For field strengths below the safety constraint of 15kAm^{-1}, only minor hysteresis loops are utilized for heating, leading to low SAR values. Magnetic nanoparticle fluids have a square dependence on the applied magnetic field (3), and are capable of generating higher heating power at lower field strengths than ferromagnetic materials. The ferrofluid reported by Hergt et al [13] with the highest heat generation has a SAR of 45Wg^{-1} at $6.5\text{kAm}^{-1}$and 300 kHz which extrapolates to 209 W g^{-1} for 14 kA m^{-1}, compared to 75 W g^{-1} at 14 kA m^{-1} for the FM magnetite sample with the greatest heat generation [11,13]. Ferrofluids are evidently capable of appreciable heat generation within the safety constraints for H_0 and f and for reasonably small sample sizes.

2.3 The Pennes Bioheat Equation

The heat flow equation for tissue, including the effects of perfusion of blood and metabolic heating is given

by the PBE:

$$\rho c \frac{\delta T}{\delta t} = \nabla \cdot (k \nabla T) = \rho_b c_b w (T - T_b) + Q_m + Q_s \qquad (5)$$

where ρ is the tissue density, c is the specific heat for the tissue, k is the thermal conductivity of the tissue, $\rho_b$is the blood density, c_b is the specific heat for blood, w is the blood perfusion rate, T_b = blood temperature, Q_m = metabolic heating, Q_s = heat added to the system from a source, such as heating due to the ferrofluid in an AC field [14]. In the case of magnetic fluid hyperthermia, the Q_s term is the energy deposition due to heating of the ferrofluid in an AC magnetic field. The heating power that determines Q_s is given by equation (3).

3 MODEL

In this research, the program Semcad X [15] will be used to solve the PBE, equation (5), for a model of the human head with a cancerous region with imbedded magnetic nanoparticles using the Finite Difference Time Domain (FDTD) method. Semcad uses the FDTD solver with volume mesh techniques applied to a 3D model in order to solve Maxwells equations in PDE form in the region of interest. The electromagnetic results are then used in the thermal simulation to solve the PBE and determine the heating. In order to perform the calculation, the user must provide dielectric, magnetic and thermal properties of all materials, the excitation for the coils (for example, the current or voltage), the AC frequency, and specify a solver (such as the FDTD solver). The current version of the model uses square Helmholtz coils to provide the AC magnetic field excitation. Square Helmholtz coils are capable of producing a magnetic field more uniform than the more commonly seen circular Helmholtz coils [16]. Densities and thermal properties of all tissue layers (skin, skull, and grey matter) and perfusion rates of the skin and skull layers were those detailed by Duck [17] and are similar to those found in the current literature [18]. The range for perfusion rates for the tumor region were those found in the literature for various grades of astrocytomas [19]. The perfusion rates for grey matter were also found in [19]. Conductivities and permittivities for the tissues at the various frequencies were obtained using the publicly available program atsf.exe [20].

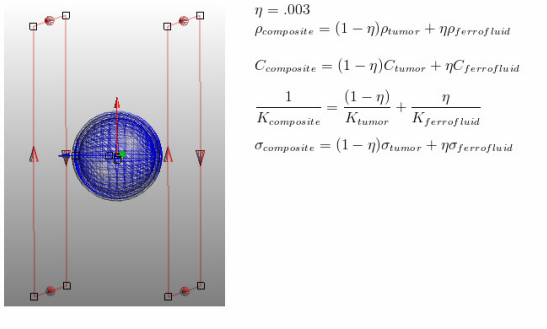

Figure 1: Square Helmholtz coils and multi-tissue layer model of human head, including a central composite region of tumor tissue and magnetic nanoparticle fluid. In both examples, the tumor/ferrofluid composite material properties were mean values of the material properties of the tumor tissue and magnetite nanoparticles, assuming homogeneity of the region. $\eta = .003$, where η is the volume fraction magnetite nanoparticles in the tumor region. 10mg of Fe per g of tumor corresponds to a volume fraction of η= .003. This is the typical dosage reported in clinical studies [21]

4 RESULTS

For both H_0= 6.5kAm^{-1} and H_0= 10 kAm^{-1} (see Figures 2 and 3) there exists a marked increase in tissue temperature near the center of the tumor region for a low rate of tumor blood perfusion. For normal perfusion rates within the tumor region, the temperature of the composite tumor/ferrofluid remains nearly that of the skin boundary layer (37^0C). Also, for the lower rate of perfusion, there is a significant increase in temperature for the composite region due to metabolic heating alone. This corresponds with clinical observations [19]. For the parameter values H_0= 6.5 kAm^{-1}, and $\chi'' = 10$, the temperature does not reach the minimum value required for apoptosis anywhere within the tissue volume. For the parameter values H_0= 10kAm^{-1}, and $\chi'' = 10$, when the rate of perfusion in the tumor region is low (30 ml/min/kg), the temperature reaches T $\approx 44.5^0$C, slightly above the upper bound for apoptotic heating. For the same parameter values, setting the perfusion rate to the same value as the surrounding grey matter lowers the heating such that the temperature does not reach the lower bound required for apoptosis.

5 ACKNOWLEDGMENT

This project was supported by grant number T32-EB004312 from the National Institute of Biomedical Imaging and Bioengineering.

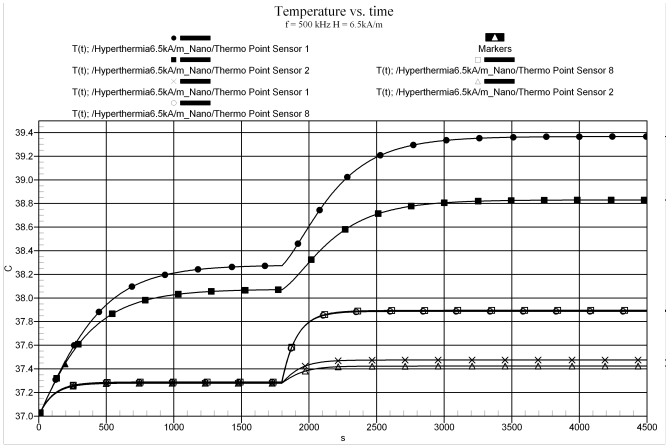

Figure 2: Heating for f = 500 kHz and H_0= 6.5kAm^{-1}. $\chi'' = 10$, an experimentally determined value for f = 500 kHz [22]. In the calculations, the low perfusion rate for the tumor region was 30 ml/min/kg, while the high value was 560 ml/min/kg, the same value as the surrounding grey matter. Metabolic heating is turned on at t= 0s and heating generated by the ferrofluid is turned on at t= 1800s. Sensor 1 is located at the center of the composite region, Sensor 2 is located at the edge of the composte region (1.5 cm from the center), and Sensor 8 is located at 4 cm from the center, inside the grey matter region). closed circle symbols, and open and closed square symbols indicate low perfusion rates, whereas the open circle, open triangle, and cross symbols indicate high perfusion rates.

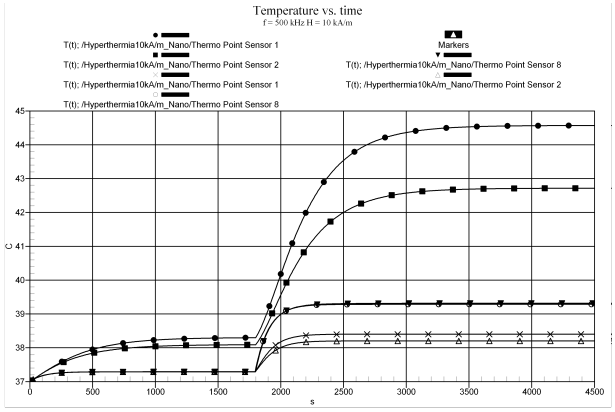

Figure 3: Heating for f = 500 kHz and H_0= 10kAm^{-1}. $\chi'' = 10$ [22]. In the calculations, the low perfusion rate for the tumor region was 30 ml/min/kg, while the high value was 560 ml/min/kg, the same value as the surrounding grey matter. Metabolic heating is turned on at t= 0s and heating generated by the ferrofluid is turned on at t= 1800s. Sensor 1 is located at the center of the composite region, Sensor 2 is located at the edge of the composte region (1.5 cm from the center), and Sensor 8 is located at 4 cm from the center, inside the grey matter region). closed symbols represent low perfusion rates, whereas the open and cross symbols indicate high perfusion rates.

REFERENCES

[1] W. Atkinson, I. Brezovich, and D. Chakraborty, IEEE Transactions on Biomedical Engineering, 31, 70-75, 1984.

[2] B. Thiesen and A. Jordan, Int. J. Hyperther., 24, 467-474, 2008.

[3] K. O' Neill, D. Fairbairn, M. Smith, and B. Poe, Apoptosis, 3, 369-375, 1998.

[4] W. Dewey, Cancer Research (Suppl.), 44, 4714s-4720s, 1984.

[5] G. Majno and I. Joris, Am. J. Pathol., 146, 3-15, 1995.

[6] E. Bonfoco, D. Krainc, M. Ankarcrona, P. Nicotera, and S. Lipton, Proc. Natl. Acad. Sci. USA, 92, 7162-7166, 1995.

[7] I. Brezovich, Med. Phys. Monogr., 16, 82, 1988.

[8] R. Hergt, S. Dutz, J. Magn. Mag. Mater., 311, 187-192, 2007.

[9] H. Sarin, A. Kanevsky, H. Wu, K. Brimacombe, et al., J. Transl. Med., 6, 80, 2008.

[10] W. Smythe, "Static and Dynamic Electricity", 375-378, McGraw-Hill, New York, 1968.

[11] Q. Pankhurst, J. Connolly, S. Jones, and J. Dobson, J. Phys. D.: Appl. Phys., 36, R167-R181, 2003.

[12] R. Rosensweig, J. Magn. Mag. Mater., 252, 370-374, 2002.

[13] R. Hergt, W. Andra, C. d'Ambly, I. Hilger, W. Kaiser, U. Richter, and H. Schmidt, IEEE Trans. Magn., 34, 3745-3754, 1998.

[14] H. Pennes, J. Appl. Physiol., 85, 5-34,1998.

[15] Semcad X Reference Manual, SPEAG -Schmid & Partner Engineering AG, http://www.semcad.com.

[16] J. Kirschvink, Bioelectromag.,13, 401 - 411,1992.

[17] F. Duck, Physical Properties of Tissue: A Comprehensive Reference Book, 1329, 329, Academic, San Diego, 1990.

[18] J. Van De Kamer, N. Wieringen, A. De Leeuw, and J. Lagendijk, Int. J. Hyperther.,17, 123 - 142, 2001.

[19] P. Vaupel, K. Friedrich, and P. Okunieff, Cancer Res., 49, 6449-6465, 1989.

[20] D. Andreuccetti, R. Fossi, and C. Petrucci, FAC-CNR, 19972007. S2919S2934, 2006.

[21] A. Jordan, R. Scholz, P. Wust , H. Fahling, et. al., Int. J. Hyperther., 13, 587-605, 1997.

[22] R. Hergt, S. Dutz , R. Mller and M. Zeisberger, J. Phys. : Condens. Matter,18, S2919 - S2934, 2006.